

Equivalent Circuit Analysis of High-Frequency Ventilators Including a New High-Impedance Flow-Interrupting Ventilator

JOSE GABRIEL VENEGAS

Abstract—The small tidal volumes (V_T) delivered to the lungs by high-frequency ventilators can be very sensitive to changes in the patient's respiratory mechanics. Analysis of a Thevenin equivalent circuit, consisting of a ventilator internal oscillatory pressure source in series with a ventilator internal impedance and a patient's respiratory impedance, reveals the need of a high-internal-impedance ventilator to minimize this V_T sensitivity problem. We present a general methodology to estimate the internal impedance of any type of ventilator. The internal impedance, at a given frequency and flow setting, is calculated from the slope of the relationship between the generated peak-to-peak pressure and the V_T delivered into a calibrated rigid tank through a varying constriction. We tested a typical high-frequency jet (HFJ) ventilator and a new high-impedance flow-interrupting (HIFI) ventilator consisting of a flow source, a rotary valve, a high-impedance expiratory tube, and a servocontrolled mean proximal airway pressure (MPAP) regulator. We found that the V_T delivered by the HIFI ventilator was independent of MPAP and decreased by 12 percent after a fivefold increase in the constriction-tank system impedance. In contrast, the V_T delivered by the HFJ ventilator decreased by 80 percent after a similar change in load. We therefore conclude that the V_T delivered by the HIFI ventilator should be significantly less sensitive to changes in patient's respiratory impedance than the V_T delivered by an HFJ ventilator.

INTRODUCTION

HIGH-frequency ventilation (HFV) is a new modality of mechanical ventilation that uses frequencies (f) (1–30 Hz) much greater than those observed in spontaneously breathing subjects and tidal volumes (V_T) similar to, or smaller than, the volume of the anatomic dead space. There is now extensive literature showing that HFV can provide enough CO_2 exchange to maintain eucapnea in normal and diseased lungs [3], [5], [17], [19], [20], [26], [13], [4]. However, the precise mechanisms of gas transport during HFV are not yet fully understood, and there are conflicting reports on the relative effects of changing the various ventilator variables [19], [20], [6], [22], [12]. The latter discrepancies are probably related to the diversity of HFV ventilators used and the lack of knowledge of their output characteristics.

In this paper, we propose a general methodology to characterize the pressure and flow output of any artificial

ventilator, using a Thevenin equivalent circuit. The interaction between the mechanical characteristics of the ventilator and those of the respiratory system determine the operating point and stability of the combined system. With this approach, we identified a set of fundamental requirements with regard to control and stability of tidal volume and gas composition, and we designed a new type of HFV ventilator that satisfies these requirements. This ventilator was tested in a lung model and its output characteristics were compared to those of a typical high-frequency jet ventilator.

THE EQUIVALENT CIRCUIT ANALYSIS

By analogy to electrical circuit analysis, which uses the Thevenin equivalent to characterize a more complex network, we can characterize the pressure-flow behavior of any artificial ventilator-patient system with the equivalent components shown in Fig. 1. The ventilator and endotracheal tube are represented by an internal oscillatory pressure source with a peak-to-peak amplitude (ΔP_I) and an internal impedance Z_I with a magnitude $|Z_I|$, the latter a function of the oscillatory frequency. In this circuit, Q represents the oscillatory flow delivered by the ventilator to the patient, and P_p is the pressure at the junction between the endotracheal tube and the patient's proximal airway.

For a sinusoidal flow, the patient's respiratory system can be represented by an impedance Z_R with a magnitude $|Z_R|$ that can be measured, at a given frequency, as the ratio of the peak-to-peak proximal airway pressure (ΔP_p) to the peak-to-peak amplitude of the oscillatory flow (ΔQ). Since ΔQ is equal to $2\pi V_T \times f$, then

$$|Z_R| = \frac{1}{2\pi f} (\Delta P_p / V_T). \quad (1)$$

The value of $|Z_R|$ can be a complicated function of f , but assuming incompressible flow and stiff airways, its order of magnitude can be estimated from a simple *RCL* model as $|Z_R| = \sqrt{R^2 + ((1/2\pi fC) - 2\pi fL)^2}$ where R is the airway resistance to flow, C is the compliance of the lungs and chest wall, and L is the inentrance of the respiratory system representing primarily the inertia of the gas in the airways. At a given frequency and for linear components, the plot of P_p versus V_T should be a linear relationship as

Manuscript received February 13, 1985; revised September 18, 1985. This work was supported in part by a fellowship from the Harvard/M.I.T. Division of Health Sciences and Technology.

The author is with the Departments of Anaesthesia and Biomedical Engineering, Massachusetts General Hospital, Boston, MA 02114.
IEEE Log Number 8407159.

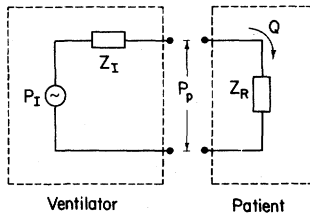


Fig. 1. Equivalent circuit of the ventilator-patient system. The ventilator is modeled by a pressure source (P_I) and a series source impedance $|Z_I|$. The patient is modeled by an impedance $|Z_R|$. The pressure across either set of terminals is P_p and the flow rate is Q .

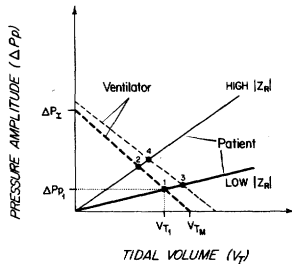


Fig. 2. Idealized relationship between the proximal airway pressure amplitude (ΔP_p) and V_T at constant frequency for the ventilator (dashed lines) and patient (solid lines). Two ventilator flow settings and two patient respiratory impedances $|Z_R|$ are illustrated. Points 1, 2, 3, and 4 represent various operating points for the system.

represented by the heavy line crossing the origin in Fig. 2. The slope of this line is equal to $2\pi f |Z_R|$ which is constant for a given f .

In the same manner, the ventilator mechanical characteristic at constant f and for a given flow setting can be described by plotting the ΔP_p versus delivered tidal volume (V_T) as represented by the heavy dashed line in Fig. 2. Notice that in one extreme, when the patient's proximal airway is totally obstructed and the delivered V_T is equal to zero, the ventilator generates the largest pressure swings with an amplitude equal to that of the internal pressure source ΔP_I ($\Delta P_p = \Delta P_I$). In the other extreme, when opened to atmosphere ($\Delta P_p = 0$), the ventilator delivers the maximum possible tidal volume (V_{Tm}). For intermediate levels of load, the V_T delivered decreases as P_p increases. The extent of this "loss" in delivered V_T is dependent on the specific ventilator design and is generally related to gas compression apparatus and breathing circuit compliance, leakage of the delivered flow toward the expiratory pathway, and/or a reduction in the net flow through the ventilator. The ratio of ΔP_I to V_{Tm} is equal to the slope of the $\Delta P_p - V_T$ curve, and its absolute value is equal to $2\pi f |Z_I|$. Under no-leak conditions, the V_T delivered by the ventilator through the distal end of the endotracheal tube must be equal to the V_T received by the patient and the value of ΔP_p at the junction must be equal for patient and ventilator. Therefore, the operating point of the ventilator-patient system is determined by the intersection between the $\Delta P_p - V_T$ curve of the ventilator and that of the patient. Thus, in this example (heavy lines in Fig. 2), the system operates at point 1 with a $V_T = V_{T1}$ and a $\Delta P_p = \Delta P_{p1}$. The operating point can be moved from 1 to 3 by adjustment of the ventilator flow setting to

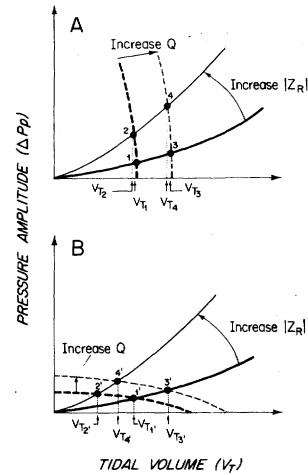


Fig. 3. Operating curves for the ventilator-patient system. High (a) and low (b) internal impedance ventilators are illustrated at two flow settings (Q) (dashed lines) and two patient impedances (solid lines). Tidal volume (V_{Ti}) at operating point (i) is determined by the intersection of the nonlinear $\Delta P_p - V_T$ curves of ventilator and patient.

shift its $P_p - V_T$ characteristic to the light dashed line (Fig. 2). The operating point could also move from 1 to 2 in response to a change in the patient's impedance, as represented by a new $\Delta P_p - V_T$ curve with a different slope (light solid line, Fig. 2). If both patient and ventilator characteristics changed, the operating point would move to 4.

Because real ventilators and real patients are usually nonlinear, it is more convenient to define Z_I and Z_R as incremental internal impedances, with magnitudes proportional to the slope of the $\Delta P_p - V_T$ curves at a given operating point i :

$$|Z|_{(i)} = \left[\frac{\partial \Delta P_p}{\partial V_T} \right]_i \cdot \frac{1}{2\pi f} \quad (2)$$

We can now compare the behavior at the same frequency of two different ventilators, one having a high internal impedance [Fig. 3(a)] and the other a low internal impedance [Fig. 3(b)]. Both graphs present $\Delta P_p - V_T$ relationships for idealized, nonlinear respirator-patient systems and show the different operating points resulting from changing the ventilator flow setting and the patient's respiratory impedance. In the same way as was previously discussed for a linear system (Fig. 2), the operating points 1, 2, 3, and 4 are obtained with the high $|Z_I|$ ventilator and 1', 2', 3', and 4' with the low $|Z_I|$ ventilator. V_{T1} is the resulting tidal volume at each operating point i (Fig. 3).

The high $|Z_I|$ ventilator has the following two practical advantages: 1) since $V_{T1} \approx V_{T2}$, the initial setting of the ventilator at a desired V_T can be made without knowing the actual characteristic of the patient, and V_T remains close to constant in spite of changes in the patient's respiratory impedance; 2) since $(V_{T3} - V_{T1}) \approx (V_{T4} - V_{T2})$, adjustment in the flow setting of the ventilator will result in a predictable change in the delivered V_T . In contrast, with a low $|Z_I|$ ventilator, the initial setting of the device

is highly dependent on the patient's unknown mechanical characteristics and thus becomes a trial-and-error process. Further, V_T can be strongly affected by a change in patient's impedance ($V_{T1} \neq V_{T2}$) and any compensatory adjustment of the ventilator's setting results in an unpredictable change in V_T [i.e., $(V_{T3} - V_{T1}) \neq (V_{T4} - V_{T2})$].

By definition, the magnitude of impedance at a given frequency can be measured directly from the peak-to-peak values of the flow and pressure signals ($\Delta Pp/\Delta Q$) only when the waveforms are purely sinusoidal. Because several types of HFV ventilators generate more complex waveforms containing several harmonics, the ratio $\Delta Pp/\Delta Q$ may not be equivalent to a true impedance. However, since our final goal is to gain information about the ability of a ventilator to deliver a net V_T under different load conditions, the general approach of plotting Pp versus V_T at a constant breathing frequency is a simple method that provides such information. So, for the sake of simplicity and by analogy to pure sinusoidal systems, we will still refer to patient and ventilator impedances even though the formal definition is not fulfilled in all HFV ventilators.

FUNDAMENTAL REQUIREMENTS OF AN HFV VENTILATOR

It is accepted that the following variables directly affect gas exchange during HFV: 1) the oscillatory flow, as characterized by $V_T \cdot f$, and the inspiratory-to-expiratory duration ratio ($I:E$); 2) the inspired gas composition; and 3) the lung volume. Peak and mean airway pressures alter gas exchange by affecting one or more of the above variables. The possible role of flow waveform (sinusoidal versus square) is presently unknown and will not be considered in the discussion. Similarly, because they are not common to all ventilators, the possible effects of the turbulence caused by a bias flow or a jet are not considered.

The effects of varying V_T and f on CO_2 transport and alveolar ventilation \dot{V}_A have been studied by several groups [19], [20], [22], [6], [12], [8], [9], yielding a relationship of the form

$$\dot{V}_A = K V_T^a f^b$$

where K is a proportionality constant, the exponent b is close to unity, and the exponent a varies between 1 and 2, depending on the study.

In practice, frequency is chosen arbitrarily and V_T is adjusted to produce and sustain adequate \dot{V}_A . Therefore, the ability to set and maintain a desired V_T independently of the patient's respiratory mechanics requires that the ventilator must have a high equivalent internal impedance.

The report [14] of potential improvements in CO_2 transport using $I:E$ ratios smaller than unity seems to justify the need for a variable $I:E$. From mechanical considerations alone, it seems clear that other benefits can be obtained from the smaller $I:E$. For example, since a small $I:E$ allows longer time for passive emptying of the lungs, the likelihood of dynamic hyperinflation and/or expira-

tory airway collapse reported to occur under certain conditions of HFV [1], [10] are minimized. Control of the inspired oxygen fraction FIO_2 is a well-established need in any ventilator. Supplying of inspired gas free of CO_2 by preventing any rebreathing is not an issue given the large V_T used in conventional ventilation. In HFV, however, small changes in rebreathing dead space can greatly improve the efficacy of ventilation [10].

From animal experiments, it is known that varying the mean lung volume (MLV) can dramatically affect O_2 exchange in HFV [11]. Therefore, it is imperative to monitor and control MLV. Relative changes in MLV can be easily detected with an impedance plethysmograph around the chest of the subject [22], but its manipulation can only be done by changes in V_T , f , $I:E$, or the mean proximal airway pressure (MPAP). Since the first three variables also affect the CO_2 gas transport, it is desirable to control the level of MLV by controlling MPAP independently of the other respiratory variables.

A HIGH-IMPEDANCE FLOW-INTERRUPTING VENTILATOR

To fulfill the above requirements, a high-impedance flow-interrupting (HIFI) ventilator was designed. The ventilator consists of: 1) a flow regulator, 2) a capacitor tank, 3) a rotary valve, 4) the breathing circuit, and 5) a feedback-controlled MPAP regulator (Fig. 4).

The flow of the respiratory gas at 3.43 bar (50 psi) is measured with a rotameter and regulated with a needle valve. The respiratory gas then enters a 7.5 l tank that serves as a capacitance. At the exit from the tank, the flow is chopped by a rotary valve and reaches the subject through an inspiratory 10 mm ID, 80 cm long tube connected to a regular 10 mm ID endotracheal tube. Mean airway pressure is measured through the lumen of a 1 mm ID air-filled catheter located 15 cm away from the tip of the endotracheal tube, at the level of the main-stem bronchi. This catheter is kept free of mucus by injecting a steady small flow of gas ($< 5 \text{ cm}^3/\text{min}$).

A MPAP regulator, feedback-controlled by the mean airway pressure signal, applies suction to a high-impedance, 2 mm ID and 30 cm long expiratory tube whose inlet is located about 1 cm proximal to the tip of the endotracheal tube [Fig. 4(b)]. The MPAP regulator varies the amount of suction applied in order to maintain the MPAP at the desired level. The response time of the MPAP regulator and catheter system ($> 2 \text{ s}$) is longer than the maximum period of HFV, and thus the system maintains a steady suction throughout the high-impedance expiratory tube.

A variable speed motor is used to rotate a valve at the desired frequency. Different valves with open-to-close duty cycles of 1:1, 1:2, and 1:4 can be mounted on the system yielding $I:E = 1-0.25$. The rotary valves have opening and closing angles of less than 5 percent of a revolution, yielding short opening and closing times that decrease as the frequency increases. This rotary valve can maintain an $I:E$ ratio of 0.25 at frequencies of 25 Hz where solenoid valves would be unable to operate.

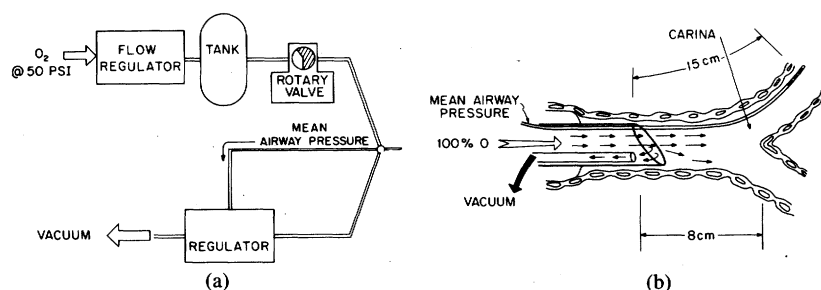


Fig. 4. (a) Schematic of the HIFI ventilator. A high-impedance flow source provides a constant flow which is interrupted by a rotary valve. Expiratory flow is controlled by a vacuum regulator such as to maintain a given mean airway pressure. (b) Schematic of the mean airway pressure sensing catheter, the high-impedance expirator (vacuum) tube, and the endotracheal tube to the central airways.

Inspiration begins when the rotary valve opens and fresh gas in injected through the main lumen of the endotracheal tube. During the inspiratory period, a fraction of the flow is being simultaneously removed through the expiratory tube. Expiration starts when the rotary valve closes, stopping the inspiratory flow while gas continues to be extracted through the expiratory tube. The combination of capacitor tank, rotary valve, and inspiratory line has an emptying time constant greater than the longest period of oscillation during HFV (> 10 s), and therefore the pressure in the capacitance tank remains approximately constant during the respiratory cycle. The rotary valve and the inspiratory tube as well as the expiratory tube present high impedances to flow so that the total pressure drop across them is much greater than the pressure fluctuations at the airway during HFV. As a result of this, the inspiratory flow and the expiratory flow remain constant throughout their respective periods.

The pressure in the rotameter is regulated at 3.4 bar, and therefore its calibration is not affected by the pressure fluctuations from the ventilator circuit. It can be calculated that gas flow for downstream pressures lower than 1.3 bar through the needle valve reaches the sonic speed (choked flow). Therefore, the flow rate through the valve for operating conditions is independent of the downstream pressure. Clearly, if gas flow were not choked at the needle valve, changes in the net impedance of the rotary valve, caused by a change in $I:E$ or f , or by adjustments in the MPAP regulator setting would affect the total flow through the system.

OUTPUT CHARACTERISTICS

Because the inspired and expired gases run through different tubes, the total inspired V_T , delivered at the tracheal end of the endotracheal tube, consists of fresh gas with a composition unaffected by the setting of the ventilator or by the patient expired gas.

Assuming that no volume is lost in gas compression in the breathing circuit, the tidal volume delivered by the HIFI ventilator can be calculated (V_{Tcalc}) from the frequency (f), the total flow (Q), and valve duty cycle ($I:E$). Since the flow rate through the expiratory tube is constant, from the conservation of mass, it must equal Q .

It follows that $V_{Tcalc} = Q \times E$ where E is the expiratory time. Since $f = (I + E)^{-1}$ where I is the inspiratory time, we have that

$$V_{Tcalc} = \frac{Q}{f \left(1 + \frac{I}{E} \right)} \quad (3)$$

METHODS

Equation (3) was tested experimentally by connecting the ventilator and endotracheal tube to a rigid 16 l test tank (dynamic compliance = 11 ml/cm H₂O). The HIFI ventilator was set at a number of predetermined combinations of Q , $I:E$, f , and MPAP and, for each setting, the peak-to-peak amplitude of the tank pressure oscillations (ΔPt) were measured from the signal trace in an oscilloscope. The ventilator settings were chosen from the following ranges: Q from 100–1000 cm³/s, f from 1–20 Hz, $I:E$ from 0.25–1, and MPAP from 0–30 cm H₂O. The tank was calibrated by rapidly introducing known values of gas and measuring the initial pressure rise with a Millar catheter tip transducer signal (resonance frequency > 20 kHz). Because the thermal time constant of the tank (> 5 s) was longer than the period of oscillation during HFV, the process was considered adiabatic during the tank calibration and the measurement of V_T . Furthermore, since the volume of the tank (V) was much greater than the maximum V_T used ($V_T/V < 0.001$ for $V_T = 150$ cm³), ΔPt is approximately a linear function of V_T :

$$V_{Tmeas} = \frac{\Delta P_t \times V}{P \times k} \quad (4)$$

where k is 1.4 for a perfect gas and P is the atmospheric pressure.

The sensitivity of V_T to changes in respiratory impedance was tested by adding a variable constriction between the distal end of the endotracheal tube and the test tank and then measuring the V_T reaching the tank. The peak-to-peak pressure fluctuations were measured with the same catheter tip pressure transducer at a site proximal to the constriction (ΔPp) and in the tank (ΔPt). The ventilator, set at $I:E = 1$, delivered a predetermined tidal volume (V_{T0}) and frequency f with the constriction fully opened.

The pressure amplitudes were measured in the proximal airway (ΔPp_0) and in the tank (ΔPt_0). The constriction was then closed in steps and both ΔPp and ΔPt were measured repeatedly. The magnitude of the constriction-tank impedance (Z_R), normalized by the tank impedance magnitude $|Z_0|$, at the same frequency and $I:E$ ratio is

$$\frac{|Z_R|}{|Z_0|} = \frac{\Delta Pp \times \Delta Pt_0}{\Delta Pt \times \Delta Pp_0} \quad (5)$$

This protocol was followed at two ventilator settings: $V_T = 80 \text{ cm}^3$ and $f = 5 \text{ Hz}$, and $V_T = 40 \text{ cm}^3$ and $f = 10 \text{ Hz}$. For comparison, a high-frequency jet (HFJ) ventilator was built and similarly tested. The jet ventilator consisted of a pressure regulator connected to a fast solenoid valve (Model 2013 by Clippard, Cincinnati, OH) with an activation time of less than 10 ms. The solenoid valve was driven with a square waveform voltage signal. The flow from the solenoid valve was delivered through a 2 mm ID 5 cm long needle placed in the center of and parallel to the endotracheal tube, 2 cm past its proximal end. A "T" connector 10 mm ID attached to the opening of the endotracheal tube allowed free gas entrainment and expiratory flow to atmosphere. No PEEP device was used in this ventilator.

RESULTS

The tank pressure signal generated by the HIFI ventilator, as recorded on an oscilloscope, showed a clear triangular waveform (Fig. 5) and $V_{T\text{meas}}$ was estimated from its peak-to-peak pressure amplitude. The traces of Fig. 5 were generated at the same $I:E = 1$ with $V_T = 80 \text{ cm}^3$ and $f = 5 \text{ Hz}$ (left), and with $V_T = 40 \text{ cm}^3$ and $f = 10 \text{ Hz}$ (right).

To illustrate the independence of V_T from MPAP, Fig. 6 presents the test tank pressure signal as the MPAP was varied from 0 to 20 cm H₂O. The amplitude of the tank pressure waveform (ΔPt), and thus delivered V_T , were not affected by the change in MPAP.

The tidal volume measured experimentally ($V_{T\text{meas}}$) and the tidal volume calculated from (3) ($V_{T\text{calc}}$) are mutually proportional (Fig. 7), as shown by the linear regression equation ($r^2 = 0.99$):

$$V_{T\text{meas}} = [1.004 \pm 0.037]V_{T\text{calc}}$$

The V_T delivered by the ventilator can be predicted with (3), with an error of less than 5 percent.

The effect of increasing the degree of constriction between ventilator and test tank was determined by plotting (Fig. 8) the tidal volume delivered across the constriction, normalized by the tidal volume measured with no constriction (V_T/V_{T0}) versus the magnitude of the impedance of the constriction-tank system, normalized by the magnitude of tank impedance with no constriction ($|Z_R|/|Z_0|$) as calculated from (5). The V_T delivered by the HIFI ventilator (solid lines) decreased by less than 12 percent for a fivefold increase of the constriction-tank system impedance. In contrast, the V_T delivered by the HFJ ventilator

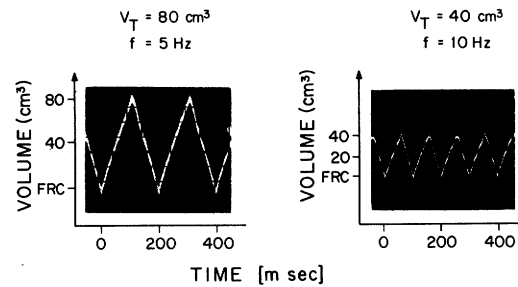


Fig. 5. Pressure excursions generated by the HIFI ventilator in a 16 l rigid test tank representing the delivered volumes with $I:E = 1$ at $V_T = 80 \text{ cm}^3$, $f = 5 \text{ Hz}$ (left), and at $V_T = 40 \text{ cm}^3$, $f = 10 \text{ Hz}$ (right).

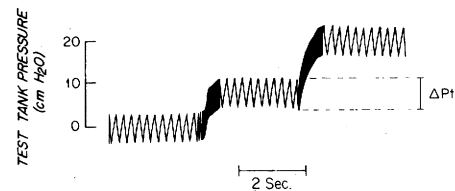


Fig. 6. Test tank pressure waveform generated by the HIFI ventilator set at $I:E = 1$, $V_T = 60 \text{ cm}^3$ and $f = 4 \text{ Hz}$. This figure shows the insensitivity of the tank peak-to-peak pressure Pt , and thus the V_T delivered, to changes in MPAP from 0 to 20 cm H₂O.

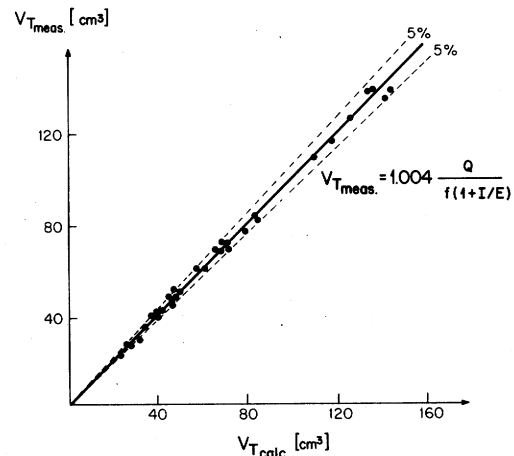


Fig. 7. Tidal volume determined from the test tank pressure excursion ($V_{T\text{meas}}$) (see Fig. 5) plotted versus tidal volume calculated from (3) ($V_{T\text{calc}}$). The regression equation and confidence limits are shown.

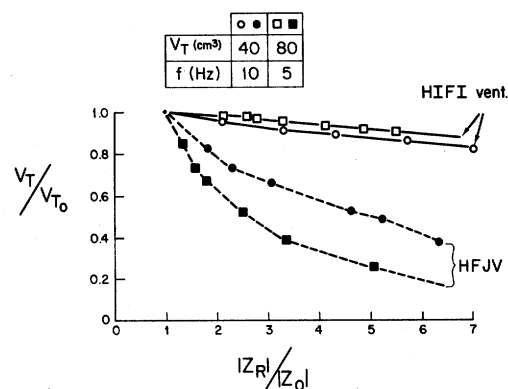


Fig. 8. Normalized tidal volume (V_T/V_{T0}) delivered to a variable constriction-tank system versus normalized "patient" impedance ($|Z_R|/|Z_0|$), using the HIFI ventilator (open symbols) and using the HFJ ventilator (solid symbols). Ventilators were set to $I:E = 1$, $V_{T0} = 80 \text{ cm}^3$, and $f = 5 \text{ Hz}$ (squares) or $V_{T0} = 40 \text{ cm}^3$ and $f = 10 \text{ Hz}$ (circles).

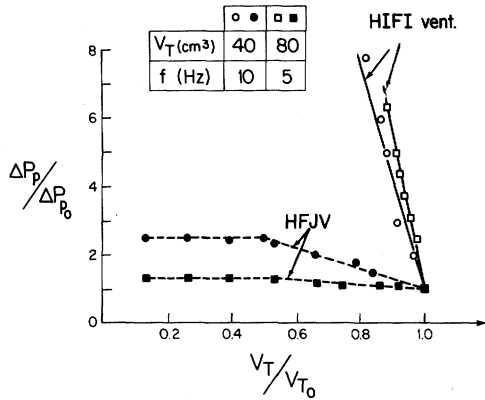


Fig. 9. Normalized peak-to-peak proximal airway pressure ($\Delta P_p/\Delta P_{p0}$) versus normalized tidal volume (V_T/V_{T0}) delivered to the tank system by an HIFI ventilator (open symbols) and by an HFJ ventilator (solid symbols). Ventilators were set to $I:E = 1$, $V_{T0} = 80 \text{ cm}^3$, and $f = 5 \text{ Hz}$ (squares) or $V_{T0} = 40 \text{ cm}^3$ and $f = 10 \text{ Hz}$ (circles).

(dashed lines) decreased by as much as 80 percent with $f = 5 \text{ Hz}$ for the same load impedance change.

The ventilator's internal impedance magnitudes can be compared by plotting the normalized proximal airway pressure amplitude ($\Delta P_p/P_{p0}$) versus the normalized tidal volume (V_T/V_{T0}) delivered (Fig. 9). From (2), the slope of these curves at any given point is equivalent to the magnitude of the ventilator internal impedance, normalized by the magnitude of the test tank impedance with no constriction ($|Z_1|/|Z_0$). ΔP_p were 3.6 cm H₂O for $V_{T0} = 40 \text{ ml}$ and 7.2 cm H₂O for $V_{T0} = 80 \text{ ml}$. At the two frequencies studied, HIFI ventilator maintained a constant slope, and thus has a constant internal impedance, even at high levels of ΔP_p . In contrast, the HFJ ventilator had an internal impedance that decreased with ΔP_p and became zero at relatively low values of ΔP_p .

Since all curves are approximately linear for $(V_T/V_{T0}) > 0.5$, internal impedance was calculated from the best fit straight lines in that range. The internal impedance of the HIFI ventilator was 44.4 and 32.6 times greater than the test tank impedance at 5 and 10 Hz, respectively. In contrast, the internal impedance of the jet ventilator was only 0.7 and 3.1 times the test tank impedance at the same frequencies. In other words, the HIFI ventilator internal impedance was 63 and 10 times greater than that of the HFJ ventilator. It follows that, at a given flow and frequency setting, in the presence of increasing load, the HIFI ventilator was able to raise its pressure amplitude to deliver the required V_T while the HFJ ventilator was not. Also, the variation in frequency had a small effect on the performance of the HIFI ventilator, but had a large effect on that of the HFJ ventilator.

DISCUSSION

In testing the HIFI ventilator and the HFJ ventilator, we used a load impedance consisting of a capacitance tank and a variable constriction. The capacitance of the tank (11 ml/cm H₂O) was ten times smaller than that of a healthy adult lung and comparable to that found in lungs with respiratory distress syndrome. The resistance of the

constriction was varied from 0 to approximately 15 cm H₂O/(l/s), a value about ten times that of a healthy lung. Therefore, the range of magnitudes of the test load impedance covered well the range of values observed clinically in lung disease. We chose the purely capacitive impedance of a test tank as a normalizing factor. Although one could argue that an impedance more similar to that of the human respiratory system, one that includes resistive and inductive elements, should be used as the normalizing impedance, the $(\Delta P_p/V_T)$ ratio of purely capacitive load is independent of flow rate and frequency. Therefore, it permits comparison performance of ventilators at different frequencies and tidal volumes. We have presented ΔP_p-V_T curves of HIFI and HFJ ventilators at a single $V_T \times f$ product and $I:E$ ratio and at two typical frequencies. However, to fully characterize the ventilators, a larger number of ΔP_p-V_T curves for various $V_T \times f$ products, $I:E$, and f should be generated. From those curves, specific circuit models of each type of ventilator could be tested to ultimately define their governing equations.

From our definition of $|Z_l|$, we can see that an HFV ventilator is equivalent to a pressure-cycled conventional ventilator when $|Z_l| = 0$ and is equivalent to a volume ventilator when $|Z_l| = \infty$. Although a true pressure HFV ventilator is relatively simple to design, a true volume HFV ventilator is not possible in practice. However, within the practical constraints, the HIFI ventilator approaches the characteristics of an ideal volume ventilator. The choked flow needle valve ensures that any variations in the rotary valve net impedance or in the MPAP are automatically balanced by an equivalent increase in the capacitance tank pressure so that, after a short delay, Q is kept constant. However, in spite of constant Q , the V_T delivered by the HIFI ventilator decreased by 12 percent after a fivefold increase in lung model impedance. This V_T loss must be attributed to gas compression and inspiratory line compliance and/or shunting of inspired gas flow to the high-impedance expiratory line. The gas compression and the tube compliance were minimized by using a relatively stiff thick-walled plastic tubing of the shortest length and diameter practical for clinical use. The loss of volume through the expiratory tube could not have been further minimized by using an expiratory tube of higher impedance, as this would require an impractically low pressure at the vacuum source.

To compare the HIFI ventilator to other HFV ventilators described in the literature, it is helpful to distinguish two main classes: 1) the high-frequency pulse generators (HFP) in which pressurized fresh gas is used to create a periodic flow waveform usually, although not necessarily, square; and 2) the high-frequency oscillators (HFO) in which the oscillatory flow is created by a reciprocating mechanism independent of the net flow of fresh gas used.

HFP are either single valved, like the HIFI or the HFJ ventilators [13], [18], or double valved like the rotary valve system used by Fletcher and Epstein [7]. The HFJ ventilator uses the high kinetic energy of a jet to entrain an additional volume of respiratory gas into the airway,

and exhalation occurs passively by the lung elastic recoil. With our experimental setup, we were able to show that the V_T delivered by a typical HFJ ventilator decreases with increasing load (Fig. 8). In clinical situations, the total V_T delivered to the lungs is difficult to measure because of the unknown volume of entrained gas. Since MPAP cannot be independently controlled in HFJ ventilation, the dynamic FRC has to be controlled with either positive end-expiratory pressure devices which affect the volume of entrained gas or with changes in $I:E$, f , or Q which affect the total alveolar ventilation. Finally, the gas entrained by the jet at the onset of inspiration is that remaining in the endotracheal tube at the end of expiration, and therefore, there is always some degree of rebreathing.

Although we did not study the V_T output characteristics of other types of high-frequency ventilators, comparisons to the HIFI ventilator characteristics can be made based on theoretical grounds and data published by others. Double-valved HFP's actively control both the inspiratory and expiratory periods of the respiratory cycle. These ventilators have two independent solenoid valves driven alternately [3], [5] or a single rotary valve that controls both inspiration and expiration [8]. Although in these systems, expiratory flow could be enhanced by adding suction to the expiratory port, typically expiration occurs passively. Because double-valved HFP's have, by nature, a high internal impedance, they permit accurate measurement and control of V_T , as has been shown experimentally [7]. Furthermore, the total inspiratory flow is made of fresh gas provided throughout the inspiratory line. However, implementation problems have not permitted their use in a clinical setting. The solenoid valve system has problems of synchrony when driven at high frequencies because of the slow response time of the valves. The rotating valve used by Epstein [7], [8] is limited to a fixed $I:E$ ratio and presents the problem of a large dead space when the valve is not located very close to the endotracheal tube.

HFO uses a reciprocating piston pump to induce the oscillatory flow in the airways. CO_2 is removed from the breathing circuit by continuous injection and extraction of an independently controlled "bias flow" of fresh gas at a site proximal to the endotracheal tube. Extraction of the bias flow occurs either passively through a large inertance "low-pass filter" tube [2], [21], [25] or actively through a high-impedance orifice [19], [20]. The second method provides for more accurate and independent control of the mean airway pressure and better ensures that a significant fraction of the oscillatory flow is not "lost" through the bias tube. The high-impedance orifice HFO system allows for direct measurement of delivered tidal volume using a carefully calibrated pneumotachograph proximal to the endotracheal tube. However, theoretically, we can expect that the HFO tidal volume will be more affected by the patient's impedance than the HIFI ventilator because in HFO, the volume of the piston chamber is added to the compressible volume of the breathing circuit. Furthermore, in HFO, the inhaled gas, depending on the bias flow rate, can be contaminated with expired gases.

In spite of the several advantages of the HIFI ventilator, it should be stressed that a proper gas conditioning system and a number of safety features must be added in order to use this ventilator clinically. Because the pressures required to drive inspiratory flow through the lumen of the endotracheal tube are much lower than those needed in HFJV, proper humidification could be achieved with a conventional type of humidifier located upstream of the capacitance tank. In this configuration, the high source impedance of the ventilator should not be affected since the compliance of the humidifier would not be added to the compliance of this breathing circuit.

In this paper, we have presented a generalized method of characterizing the V_T output of any HFV ventilator. The method consists of plotting the ventilator's $\Delta P_P - V_T$ curves at constant f and Q settings, and calculating the normalized internal impedances from the slope of the curves at a given operating point. We have designed and tested a high-impedance flow-interrupting (HIFI) ventilator with servocontrolled MPAP independent from V_T , f , and $I:E$. The HIFI ventilator delivers a predictable V_T of 100 percent fresh gas, nearly independent of the patient's respiratory impedance or MPAP. Therefore, the HIFI ventilator permits well-controlled physiological data collection. We have, in fact, successfully ventilated a number of dogs [22], [23] studying the regional distribution of ventilation during HFV by imaging the washout of nitrogen-13 with a positron camera.

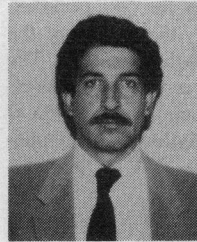
ACKNOWLEDGMENT

The author thanks Prof. A.H. Shapiro, Dr. E. Trautman, and Dr. D. Carley for their helpful suggestions.

REFERENCES

- [1] W. C. Beamer, D. S. Prough, R. L. Royster, and J. C. Johnson, "High frequency jet ventilation produces auto-PEEP (Abstract)," in *Proc. Memorial Sloan Kettering Int. Symp. High Frequency Ventilation*, C. Carlson, Ed. New York: 1983, p. 63.
- [2] D. J. Bohn, K. Miyasaka, B. Marchak, W. K. Thompson, A. B. Froese, and A. C. Bryan, "Ventilation by high frequency oscillation," *J. Appl. Physiol., Resp. Environ. Exercise Physiol.*, vol. 4, pp. 710-716, 1980.
- [3] J. B. Bunnell, J. H. Karlson, and D. C. Shannon, "High frequency a positive pressure ventilation in dogs and rabbits," *Amer. Rev. Resp. Dis. (suppl.)*, vol. 117, p. 289, 1978.
- [4] G. C. Carlon, R. C. Kahn, W. S. Howland, R. Cole, Jr., and A. D. Turnbull, "Clinical experience with high frequency jet ventilation," *Crit. Care Med.*, vol. 9, no. 1, pp. 1-6, 1981.
- [5] J. R. Custer and D. C. Shannon, "High frequency ventilation enhances oxygenation and alveolar ventilation at reduced airway pressures in animal model of pulmonary edema," *Amer. Rev. Resp. Dis. (suppl.)*, vol. 119, p. 226, 1979.
- [6] J. Dietz, N. Macintyre, and N. Leadherman, "Gas transport and ventilation distribution as a function of tidal volume and breathing frequency in a mechanical lung model (Abstract)," in *Proc. Memorial Sloan-Kettering Int. Symp. High Frequency Ventilation*, C. Carlon, Ed. New York: 1983, p. 55.
- [7] P. R. Fletcher and R. A. Epstein, "Constancy of physiological dead space during high-frequency ventilation," *Resp. Physiol.*, vol. 47, pp. 38-49, 1982.
- [8] P. R. Fletcher, M. F. Epstein, and R. A. Epstein, "A new ventilator for physiologic studies during high-frequency ventilation," *Resp. Physiol.*, vol. 47, pp. 21-37, 1982.
- [9] J. J. Fredberg, "Augmented diffusion in the airways can support pulmonary gas exchange," *J. Appl. Physiol.: Resp. Environ. Exercise Physiol.*, vol. 49, pp. 323-328, 1980.

- [10] N. Gavrieli, J. Solway, R. Kamm, and A. H. Shapiro, "Effect of endotracheal tube on CO₂ elimination by small volume high frequency ventilation in dogs (Abstract)," *Amer. Rev. Resp. Dis.*, vol. 125, no. 2, p. 232, 1982.
- [11] P. Hamilton, A. Onayemi, H. Smyth, J. Gillan, E. Cutz, A. Froese, and A. Bryan, "Comparison of conventional and high-frequency ventilation: Oxygenation and lung pathology," *J. Appl. Physiol.: Resp. Environ. Exercise Physiol.*, vol. 55, no. 1, pp. 131-138, 1983.
- [12] W. C. Jaeger and U. Kurzweg, "The dispersion of gas in high frequency ventilation (Abstract)" in *Proc. Memorial Sloan-Kettering Int. Symp. High Frequency Ventilation*, C. Carlon, Ed. New York: 1983, p. 61.
- [13] M. Klain and R. B. Smith, "High frequency percutaneous jet ventilation," *Crit. Care Med.*, vol. 5, pp. 280-287, 1977.
- [14] W. H. Paloski, P. S. Barie, R. J. Mullins, and J. C. Newell, "Effects of inspiratory to expiratory time ratio on carbon dioxide elimination during high frequency jet ventilation," *Amer. Rev. Resp. Dis.*, vol. 131, pp. 109-114, 1985.
- [15] T. H. Rossing, A. S. Slutsky, J. Lehr, P. Drinker, R. D. Kamm, and J. M. Drazen "Tidal volume and frequency dependence of carbon dioxide elimination by high-frequency ventilation," *N. Eng. J. Med.*, vol. 305, pp. 1375-1397, 1981.
- [16] T. H. Rossing, A. S. Slutsky, R. H. Ingram, Jr., R. D. Kamm, A. H. Shapiro, and J. M. Drazen, "CO₂ elimination by high frequency oscillation in dogs—Effects of histamine infusion," *J. Appl. Physiol.: Resp. Environ. Exercise Physiol.*, vol. 53, pp. 1256-1262, 1982.
- [17] U. Sjostrand, "Review of the physiologic rationale for the development of high frequency positive pressure ventilation—HFPPV," *Acta Anaesthesiol. Scand. Suppl.*, vol. 64, pp. 7-27, 1977.
- [18] —, "High-frequency positive pressure ventilation (HFPPV): A review," *Crit. Care Med.*, vol. 8, no. 3, pp. 345-364, 1980.
- [19] A. S. Slutsky, J. M. Drazen, R. H. Ingram, Jr., R. D. Kamm, A. H. Shapiro, J. J. Fredberg, S. H. Loring, and J. Lehr, "Effective pulmonary ventilation with small volume oscillations at high frequency," *Science*, vol. 209, pp. 609-611, 1980.
- [20] A. S. Slutsky, R. D. Kamm, T. H. Rossing, S. H. Loring, J. Lehr, A. H. Shapiro, R. H. Ingram, Jr., and J. M. Drazen, "Effects of frequency, tidal volume and lung volume on CO₂ elimination in dogs by high frequency (2-30) Hz, low tidal volume ventilation," *J. Clin. Invest.*, vol. 68, pp. 1474-1484, 1981.
- [21] E. R. Schmid, T. Knopp, and K. Rehder, "Inter-regional mixing during high frequency oscillation (HFO)," *Physiologist*, vol. 23, p. 108, 1980.
- [22] J. G. Venegas, "Efficiency and distribution of high frequency ventilation," Ph. D. dissertation, M.I.T., Cambridge, 1983.
- [23] J. G. Venegas, J. Custer, B. Hoop, and C. Hales, "Distribution of ventilation at high frequency (Abstract)," *Fed. Prod.*, vol. 8633, p. 1746, Mar. 1982.
- [24] J. G. Venegas and M. Venegas, "Pulsos reversos de presion. Nueva alternativa para el tratamiento de las enfermedades pulmonares obstructivas cronicas," *Tribuna Medica*, vol. 60, no. 8, pp. 33-42, 1979.
- [25] K. Wright, R. K. Lyrene, W. E. Troug, T. A. Standaert, J. Murphy, and D. E. Woodrum, "Ventilation by high-frequency oscillation in rabbits with oleic acid lung disease," *J. Appl. Physiol.: Resp. Environ. Exercise Physiol.*, vol. 50, pp. 1056-1060, 1981.



Jose G. Venegas was born in Casabe, Colombia, on November 29, 1951. He received the Ingeniero Mecanico degree from the University of Los Andes, Bogotá, Colombia, in 1973, the M.Sc. degree in production engineering and management from the University of Aston, Birmingham, England, in 1975, and the Ph.D. degree in medical engineering and medical physics from the Harvard-M.I.T. Division of Health Sciences and Technology, Cambridge, in 1983.

From 1975 and 1978 he was an Associate Professor in the Department of Mechanical Engineering, University of Los Andes, Bogotá, and conducted research in the area fluid mechanics of the cerebrospinal fluid and optimal design of shunts to treat hydrocephalus. His Ph.D. dissertation was devoted to the measurement, *in vivo*, of the overall gas transport and regional distribution of alveolar ventilation during high-frequency ventilation using positron imaging techniques.

Dr. Venegas holds U.S. and U.K. patents on a respiration-assisting device and was awarded on two occasions the Colombian most prestigious yearly science prize, Alejandro Angel Escobar (1974 and 1977) and the Harold Lamport Award from the Biomedical Engineering Society (1984). Since 1983 he has continued studies in the areas of respiratory gas transport and lung mechanics as a Research Associate in the Departments of Anaesthesia and Biomedical Engineering, Massachusetts General Hospital, Boston. He is currently an Instructor in Anaesthesia (Bioengineering) at the Harvard Medical School, Boston.